Large area nanopatterning of alkylphosphonate self-assembled monolayers on titanium oxide surfaces by interferometric lithography

ARTICLE *in* NANOSCALE · MARCH 2011

Impact Factor: 7.39 · DOI: 10.1039/c0nr00994f · Source: PubMed

6 AUTHORS, INCLUDING:

Steven Brueck
University of New Mexico
453 PUBLICATIONS **8,352** CITATIONS

SEE PROFILE

Nanoscale

www.rsc.org/nanoscale

Volume 3 | Number 6 | June 2011 | Pages 2345–2644

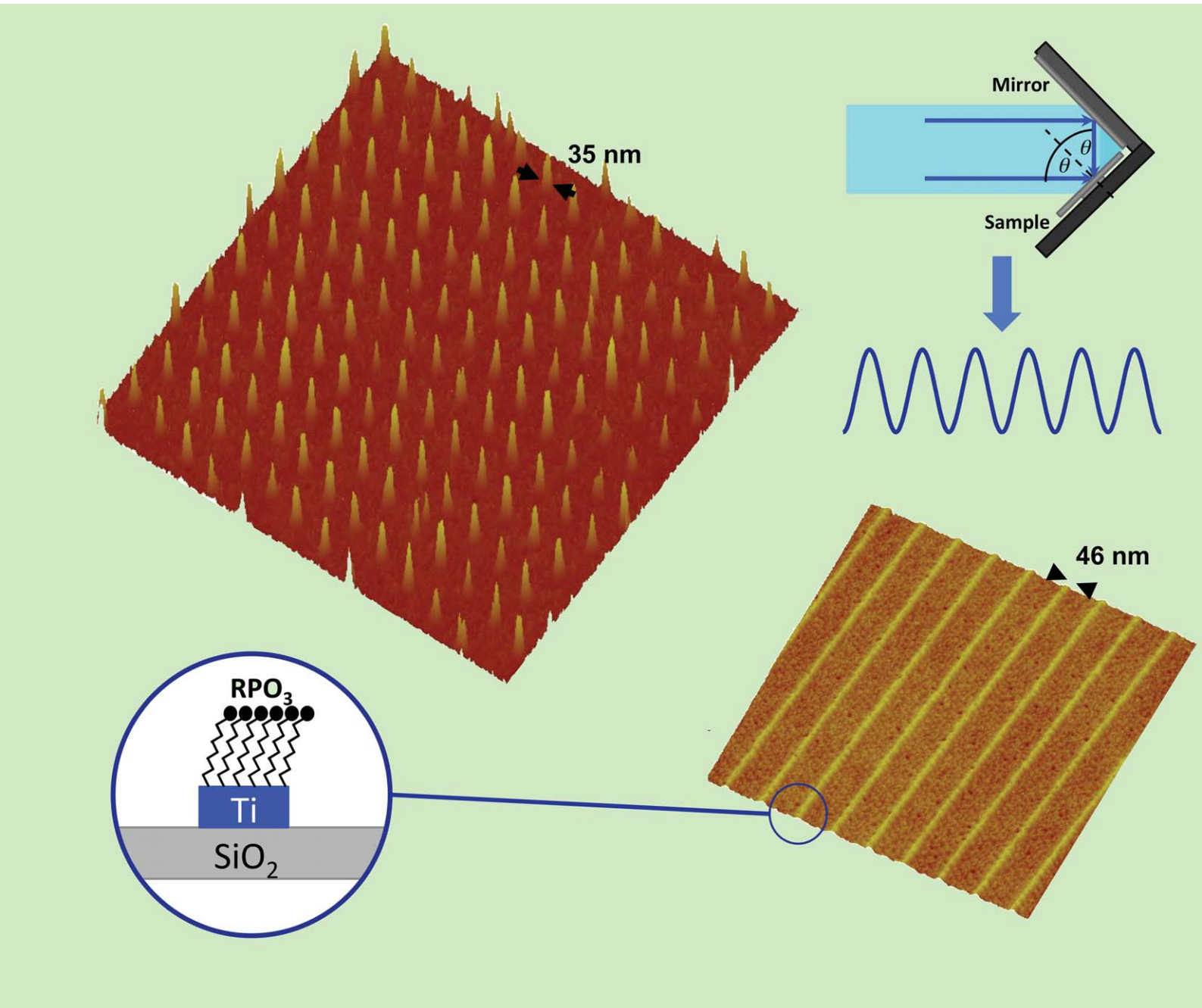

ISSN 2040-3364

COVER ARTICLE
Leggett *et al.*
Large area nanopatterning of alkylphosphonate self-assembled monolayers on titanium oxide surfaces by interferometric lithography

HOT ARTICLE
Chen *et al.*
Blending of $HAuCl_4$ and histidine in aqueous solution: a simple approach to the Au_{10} cluster

RSC Publishing

Nanoscale

Dynamic Article Links

Cite this: *Nanoscale*, 2011, **3**, 2511

www.rsc.org/nanoscale

PAPER

Large area nanopatterning of alkylphosphonate self-assembled monolayers on titanium oxide surfaces by interferometric lithography

Getachew Tizazu,[a] Osama El-Zubir,[a] Steven R. J. Brueck,[b] David G. Lidzey,[c] Graham J. Leggett*[a] and Gabriel P. Lopez*[de]

Received 16th December 2010, Accepted 17th February 2011
DOI: 10.1039/c0nr00994f

We demonstrate that interferometric lithography offers a fast, simple route to nanostructured self-assembled monolayers of alkylphosphonates on the native oxide of titanium. Exposure at 244 nm using a Lloyd's mirror interferometer caused the spatially periodic photocatalytic degradation of the adsorbates, yielding nanopatterns that extended over square centimetre areas. Exposed regions were re-functionalised by a second, contrasting alkylphosphonate, and the resulting patterns were used as templates for the assembly of molecular nanostructures; we demonstrate the fabrication of lines of polymer nanoparticles 46 nm wide. Nanopatterned monolayers were also employed as resists for etching of the metal film. Wires were formed with widths that could be varied between 46 and 126 nm simply by changing the exposure time. Square arrays of Ti dots as small as 35 nm ($\lambda/7$) were fabricated using two orthogonal exposures followed by wet etching.

Introduction

Self-assembled monolayers (SAMs),[1–5] formed by the spontaneous assembly of adsorbates from dilute solution onto solid surfaces, have attracted interest for many applications in nanoscience and technology.[6] The most widely studied SAMs are those formed by the adsorption of alkylthiolates onto gold surfaces,[3–5] and by the adsorption of alkylsilanes onto silicon dioxide surfaces.[1,2] However, alkylphosphonic acids also assemble onto the oxides of aluminium, titanium and niobium to form close-packed monolayers that exhibit closer packing than films formed from either alkylthiolates or alkylsilanes,[7–10] and superior oxidative stability[11,12] to alkylthiolate SAMs. Given the technological importance of titanium dioxide, alkylphosphonates are expected to assume increasing importance in the future.

Titania surfaces are important in many areas of science and technology. They are important in a range of photonic applications,[13–16] and are used in the dye-sensitised solar cell (or Grätzel cell).[17] Nanostructured Ti oxides are used to optimise the interfacial area and maximise electronic transfer from the dye to the semiconductor. TiO_2 has attracted interest for the photocatalytic generation of hydrogen from water.[18] In nanoparticulate TiO_2, control of nanocrystal size presents one means to control the band gap,[19] necessary to optimise the catalytic activity. Nanoparticulate gold supported on TiO_2 has been reported to have catalytic activity in water splitting, and to have potential for use in photovoltaic devices.[20] Titania surfaces exhibit a strong photocatalytic effect: absorption of UV light creates electron–hole pairs at the oxide surface leading to the oxidative breakdown of organic matter.[21,22] This has been exploited in a variety of applications including, for example, use in self-cleaning glass[23] and in the breakdown of industrial pollutants.[24]

While there has been some interest in patterning molecular adsorbates on oxide surfaces, most attention has been focused on alkylsilane films and comparatively little effort has been devoted to patterning alkylphosphonate SAMs. Goetting *et al.* used microcontact printing to pattern phosphonic acids on alumina.[25] At the nanometre scale, Gadegaard used electron beam lithography to pattern alkylphosphonates.[26] Near-field optical techniques were used to pattern alkylphosphonate SAMs on alumina and to etch 100 nm structures into the underlying metal.[27] The mechanism was suggested to be photolytic scission of the P–C bond. On TiO_2, organic adsorbates are rapidly degraded when in close proximity to TiO_2 surfaces, and this may be exploited in patterning.[27–31]

While electron beam lithography is capable of yielding very high resolution, it is nevertheless difficult to access for many researchers, requiring expensive infrastructure and skilled technical staff. Moreover, it is not well-suited to the patterning of large areas. Scanning-probe-based lithography techniques are more readily accessible, but in general, are slow and do not

[a]*Department of Chemistry, University of Sheffield, Brook Hill, Sheffield, S3 7HF, UK. E-mail: Graham.Leggett@shef.ac.uk*
[b]*Center for High Technology Materials, University of New Mexico, Albuquerque, NM, 87106, USA*
[c]*Department of Physics and Astronomy, University of Sheffield, Hounsfield Road, Sheffield, S3 7RH, UK*
[d]*Center for Biomedical Engineering and Dept. of Chemical and Nuclear Engineering, University of New Mexico, Albuquerque, NM, 87131, USA*
[e]*Department of Biomedical Engineering, Duke University, Durham, NC, 27708, USA. E-mail: gl52@duke.edu*

enable fabrication over macroscopically extended areas. Parallel probe instruments have been reported,[28–30] but are not widely available and require specialized expertise. In the present paper, we explore an alternative approach, interferometric lithography (IL), which requires inexpensive apparatus (a suitable laser and a few lenses), and which should be capable of adoption by laboratories not possessing any other infrastructure for nanofabrication.

Interferometric methods[31,32] have been long known in semiconductor device fabrication, and provide a convenient and effective means for exposing photoresist at high spatial resolution. A wide range of geometries is possible, providing an enormous variety of interference schemes and conferring a high degree of control over morphology. Moreover, compared to electron beam lithography, the infrastructure requirements for IL are very modest. Despite these are attractive features, IL has been surprisingly little used to fabricate molecular nanostructures. A small number of reports has described the application of IL to organic monolayers. Freibel *et al.* used an excimer laser ($\lambda = 193$ nm) to form comparatively large structures with a period of 532 nm in alkylthiolate SAMs, probably by degradation of the alkyl chain.[33] Geldhauser used a 157 nm laser to generate surface energy patterns by a similar route.[34] Schuh *et al.* used IL to form continuous gradients of polymer brush density, with feature sizes as small as 100 nm.[35] Even smaller structures were fabricated by Turchanin *et al.*,[36] who used extreme-UV radiation from a synchrotron light source to modify alkylthiolate monolayers with photosensitive nirobenzyl terminal groups and achieved a period as small as 60 nm. The objective of the present study is to examine the capability provided by a simple bench-top apparatus for conducting IL of alkylphosphonate SAMs on titania surfaces, using photocatalytic degradation of the adsorbate. The possibility of using IL-patterned alkylphosphonate films to pattern nanoparticle deposition and to fabricate Ti nanostructures has been investigated.

Materials and methods

Titanium (99.9%) was obtained from Goodfellow (Cambridge, UK). Aminobutylphosphonic acid was purchased from Sigma Aldrich (Poole, UK) and octadecylphsophonic acid was obtained from Alfa Aesar (Heysham, UK). Ethanol (HPLC grade) and toluene were obtained from Fisher Scientific Ltd. (Loughborough, UK).

Glass slides and glass vials were thoroughly cleaned by soaking them in piranha solution (30% hydrogen peroxide solution and concentrated sulfuric acid in the ratio of 3 : 7) for 1 h, rinsing them seven times with deionized water and drying them in an oven. **Caution**: piranha solution is a very aggressive oxidising agent and may detonate on contact with organic materials. Titanium dioxide substrates were prepared by evaporating *ca.* 15–20 nm of titanium onto glass slides at a rate of 0.05 nm s^{-1}. An Edwards Auto306 vacuum coating system was used for Ti deposition. Following deposition, the evaporator was allowed to cool, before venting to dry nitrogen. The slides were then exposed to the laboratory atmosphere for 20 min, allowing formation of the native oxide film and surface hydroxylation (a necessary precursor to SAM formation). SAMs were formed by immersion of the substrates in a 1 mM ethanolic solution of the appropriate phosphonic acid for 48 h.

Interferometric lithography was carried out using a Coherent Innova 300C FreD frequency-doubled argon ion laser, emitting at a wavelength of 244 nm with a maximum power of 100 mW.

Refunctionalization of UV modified octadecylphosphonate monolayers was carried out by immersion of the samples in a 0.1 mM aqueous solution of aminobutyl phosphonic acid for 30 min. Aldehyde nanoparticle attachment was carried out by immersing amine functionalized samples in a 0.1 M 2-(*N*-morpholino) ethanesulfonic acid (MES) buffer of pH 6.1 that contains 10 μL of aldehyde modified polystyrene nanospheres (diameter 200 nm, Invitrogen) for 30 min.

Etching was carried out by immersion of photopatterned samples in a mixture of 10 mL conc. sulfuric acid and 5 mL of hydrogen peroxide that had cooled for 20 min. The etching time was 40 min.

Results and discussion

Methodology

Fig. 1 shows schematically the Lloyd's mirror arrangement used in the present work.[31] A laser beam was expanded to illuminate an area of *ca.* 1 cm^2, and directed towards a sample positioned at an angle 2θ from a mirror. Half the beam interacted directly with the sample, while the other half struck the mirror and was reflected onto the sample, where it interfered with the first half of

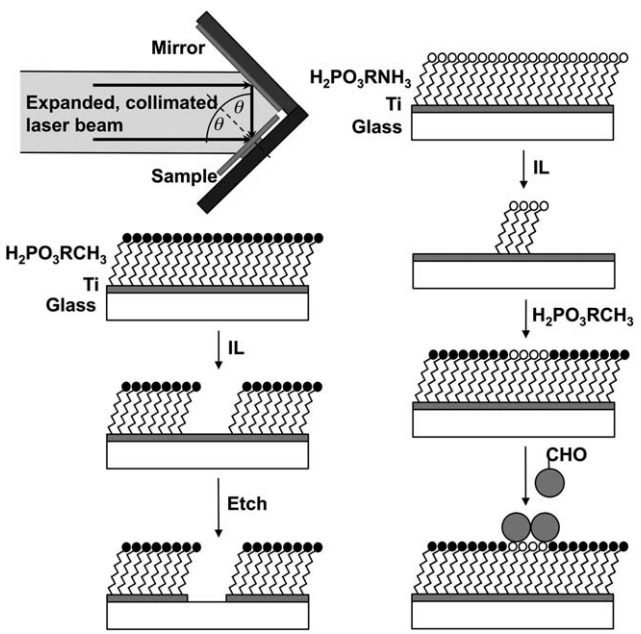

Fig. 1 Schematic diagrams showing the Lloyd's mirror configuration used to carry out interferometric lithography (top left) and the steps involved in the lithographic processing of self-assembled monolayers of alkylphosphonates on titanium oxide (remainder of figure). Left: fabrication of metal nanostructures, by exposure of a methyl-terminated SAM followed by etching in "piranha" solution. Right: patterning of amine-functionalized SAM followed by passivation of exposed regions with a methyl-functionalized adsorbate and attachment of aldehyde-functionalized polymer nanoparticles.

the beam, producing an interference pattern with a period $\lambda/2n\sin\theta$. To photopattern SAMs of alkylphosphonates (see Fig. 1) adsorbed onto the native oxide of titanium, UV exposure (using light from a frequency-doubled argon ion laser, $\lambda = 244$ nm) led to the photocatalytic degradation[21,22,29,31,40] of the adsorbate layer.[37,38] The oxide surface was then either re-functionalized with a second phosphonic acid possessing a contrasting terminal group[38] (for example, an amine terminated phosphonic acid, that could be derivatized by an aldehyde-functionalized polymer nanoparticle), or etched using "piranha solution", a mixture of concentrated sulfuric acid and hydrogen peroxide that eroded the metal oxide in the exposed regions and also the underlying metal (Fig. 1).

Patterning of monolayers on titanium oxide

SAMs were formed by the adsorption of octadecylphosphonic acid (ODPA) on the native oxide of titanium using established procedures.[38] XPS analysis confirmed the purity of the films (data not shown), in agreement with previously published work.[38] SAMs were exposed using IL. The resulting patterns were characterized using friction force microscopy (FFM),[39–41] a variant of atomic force microscopy (AFM) in which lateral deflections of the cantilever are measured. Fig. 2a shows a sample that has been exposed for 1 min at a laser power of 50 mW cm^{-2}. For comparative purposes, conventional photoresists have sensitivities of 10–50 mJ cm^{-2}. Alternating bands of bright and dark contrast were observed, with a period of 180 nm. The unmodified regions of the sample exhibited dark contrast because the regions occupied by intact adsorbates have a low surface free energy, while the modified regions, with a full width at half maximum (FWHM) of 120 nm, exhibited bright contrast because in those areas, the hydrophilic substrate has been revealed. The AFM probe adheres more strongly to the high-surface-energy regions, causing a higher rate of energy dissipation and hence a larger frictional force.[42] Fig. 2b shows a sample that has been exposed a second time, following rotation of the sample through 90°. The second exposure yielded orthogonal lines of exposed material, with the intact areas forming an array of dark spots in the resulting FFM image. The period of the resulting structure was 180 nm and the FWHM of the dark spots was 60 nm.

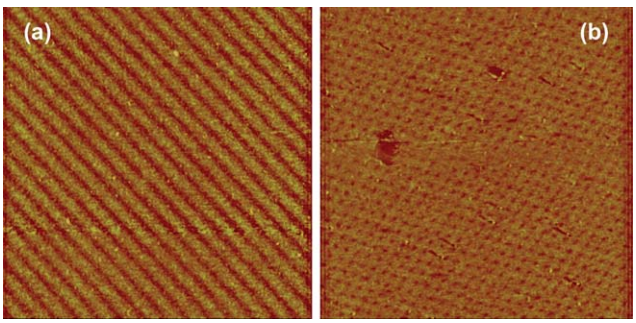

Fig. 2 Patterns formed in octadecylphosphonic acid monolayers on titanium oxide by IL-initiated photocatalytic patterning. Image sizes: (a) 4.4 × 4.3 μm^2, z-contrast range 0–0.2 V, dark to bright; (b) 6 × 6 μm^2, z-contrast range 0–0.5 V, dark to bright.

By over-exposing the sample it was possible to "whittle" the unexposed regions until structures resulted that were much narrower than might be expected for a diffraction-limited technique.[43] Fig. 3a shows schematically how this is accomplished. At low exposures, only narrow regions at the peaks of intensity in the interference pattern yield full modification of the monolayer. As time progresses, the region that has been fully modified by the catalytic degradation process increases in width, effectively spreading outwards from the central maximum of the interference pattern in the direction of the arrow in Fig. 3a. The approach is analogous with methods for "thinning" that are widely used to reduce feature size in electronic device fabrication by conventional photolithography, but utilising a different process. Because of the extremely thin nature of the monolayer, the "whittling" process proceeds in a highly uniform way within the surface plane enabling very precise control over feature sizes. Fig. 3b illustrates this process, showing structures formed by "whittling" an aminobutyl phosphonic acid (ABPA) monolayer, and then refunctionalizing the eroded regions using ODPA. The surface has then been functionalized by immersion in a solution of 40 nm-diameter aldehyde-functionalized latex particles, which attach to the amine-functionalized regions *via* the formation of an imine bond. The tapping mode AFM topographical image in Fig. 3b shows lines of bright contrast, where latex particles have attached to intact ABPA molecules, separated by broad bands where the amine-terminated adsorbate has been removed and replaced by ODPA. The bright features exhibit a mean line width of 46 nm, consistent with the formation of a feature only one particle wide. Note that while the line edge roughness appears to be significant in Fig. 3, this is in fact due to the approximately spherical shape of the polymer particles, and the fact that their diameters are close to the line width.

Fabrication of metal nanostructures

"Photochemical whittling" of the monolayer resist provides an exceptionally simple and readily controlled route to the fabrication of metal nanostructures. Monolayers of ODPA on

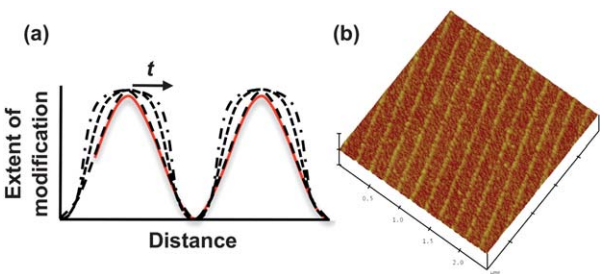

Fig. 3 (a) Two coherent, interfering laser beams yield a sinusoidal interference pattern. When used to expose a photosensitive material, modification proceeds to completion first in the region exposed to the maximum of intensity, and the fully modified zone then spreads with time in the direction of the arrow enabling structures to be "whittled" to dimensions much less than $\lambda/4$. (b) 46 nm lines of polymer nanoparticles formed by IL exposure of aminobutylphosphonic acid monolayers on titanium oxide, followed by immersion in a solution of actadecylphosphonic acid (to passivate the exposed regions) and a solution of aldehyde-functionalized latex nanoparticles. Image size: 2.4 × 2.4 μm^2; z-scale range 0 – 60 nm dark to bright contrast.

titanium oxide were exposed using IL and subsequently etched using "piranha solution", a mixture of 30% hydrogen peroxide solution and concentrated (95%) sulfuric acid in the ratio 3:7. Piranha solution is a known etchant for Ti. The etchant was expected to erode the metal from regions where the SAM had been photocatalytically degraded, while the regions where the SAM remained intact were expected to be masked. Fig. 4a shows a sample that has been patterned in a single exposure. Well-defined, unbroken ridges—Ti nano "wires"—of uniform width were observed. The FWHM was 46 nm and the wires extended across an area of 0.5 cm^2. The line edge roughness is much lower than in Fig. 3, because it is now defined by the perimeter of the oxidized region of the molecular monolayer

By carrying out two orthogonal exposures, and subsequently etching the sample in Piranha solution, it was possible to fabricate Ti nanodots. Fig. 4b shows a representative example. The feature sizes are even smaller than those in Fig. 4a: the cross-section shown in Fig. 4c shows that the full width at half maximum height for these structures is only 35 nm (*ca.* $\lambda/7$). The native oxide of Ti is thin, in the range 1–3 nm,[44,45] so the majority of the volume of the nanodots in Fig. 4 probably consists of metallic Ti. Direct verification of this was difficult because of the very small size of the structures. However, XPS data for macroscopic, unpatterned samples, masked by SAMs but exposed to the etch solution, confirmed the predominance of metallic Ti in the substrate.

The width of the features could be controlled readily by varying the UV exposure time. Fig. 5 shows the variation in the line width for samples exposed at a laser power of 50 mW. The linewidth could be controlled in a reproducible fashion between 126 nm and 46 nm simply by varying the exposure time. After 1 min, the height difference between the exposed and masked regions was 16 nm, the full thickness of the metal film. When the exposure was increased beyond this time, there was a negligible change in the line width.

Piranha solution is a strong oxidising agent. To confirm that the SAM was not being removed during the etching process, measurements were made of the contact angles of unpatterned monolayers that had been exposed to piranha solution (Fig. 6). The contact angle decreased to *ca.* 60° over a period of 60 min,

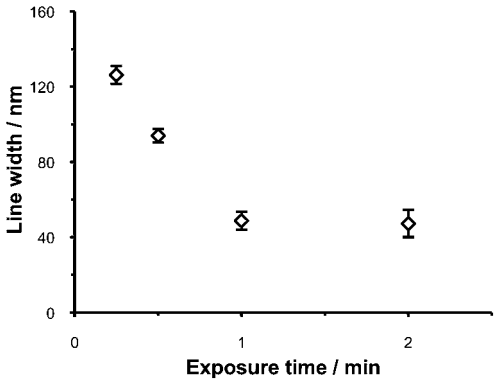

Fig. 5 Variation in line width (FWHM) as a function of UV exposure time for Ti nanowires formed by a single exposure followed by etching in piranha solution.

indicating some modification of the monolayer structure. Analysis of XPS spectra showed that the C1s signal intensity was little changed, even after one hour exposure to the etch solution although the P2p intensity was reduced. Probably, there was some removal of adsorbates during this period, but the persistence of a significant P2p signal even after one hour of immersion suggests that a substantial fraction of the monolayer remains in place at the surface. It was concluded that the rate of dissolution of the unprotected oxide greatly exceeds the rate of degradation of the organic film. Selection of the appropriate etch time thus enables the use of the SAM as a resist for etching of the underlying metal. Over-etching of the patterned structures by the use of exposures significantly longer than 40 min led to complete removal of the SAM resist and subsequent removal of the Ti film.

The potential for using such a simple fabrication to prepare macroscopically extended arrays (the area was ~0.5 cm^2 in the present case, but this may readily be expanded to much larger areas) is substantial. For example, Ti could be replaced by Au or Ag and a thiol used as a resist to yield plasmonically active structures suitable for biosensing applications[46] (photopatterning of SAMs has been used in conjunction with near-field exposure and mild wet etches to yield nanostructures of comparable resolution). Moreover, IL also offers the potential to

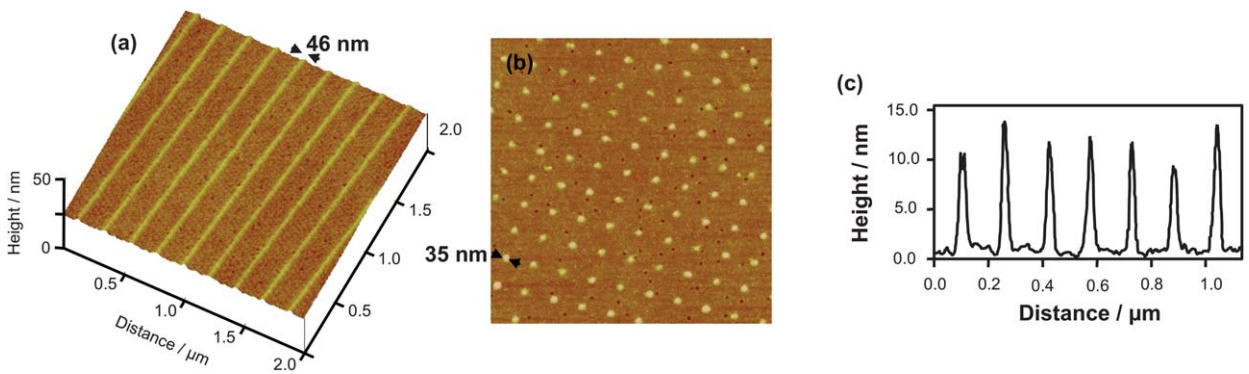

Fig. 4 Use of photochemical "whittling" to fabricate metal nanostructures, by first exposing a SAM of octadecylphosphonic acid on titanium oxide using IL and then subsequently immersing the sample in a solution of Piranha solution. (a) Tapping mode topographical image of Ti lines formed in a single exposure. (b) Variation in the line width with the IL exposure time for samples that have been etched following a single exposure. (c) A 2 × 2 μm^2 tapping mode height image of an array of Ti nanodots formed by two orthogonal IL exposure followed by etching (*z*-contrast range 0–30 nm, dark to bright). (d) A line section through (c) revealing a full width at half maximum height of only 35 nm.

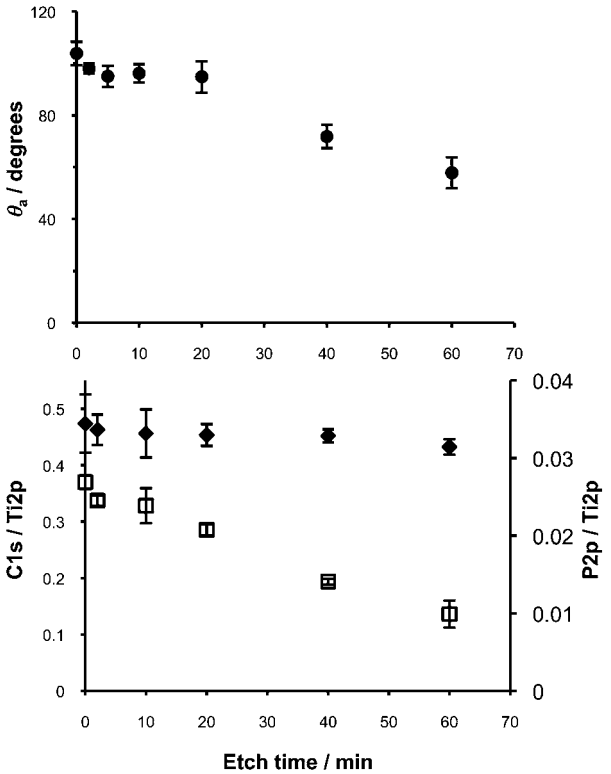

Fig. 6 Top: variation in contact angle as a function of etch time for unmodified APA SAMs immersed in piranha solution. Bottom: variation in C1s/Ti2p (diamonds) and P2p/Ti2p (squares) relative XPS intensity ratios with time of immersion in piranha solution for unmodified APA SAMs.

fabricate a wide range of structures by varying the interference arrangement in a controllable fashion (*e.g.* multiple beams, or multiple exposures, at variable angles).

Conclusions

Interferometric lithography provides a rapid, simple method for patterning self-assembled monolayers of alkylphosphonates on Ti. Exposure of samples to UV light in a Lloyd's mirror interferometer causes spatially defined photocatalytic degradation of the adsorbates. The process may be controlled with great precision. Molecular patterns may be fabricated by replacing degraded material by a contrasting alkylphosphonate. Amine functionalised lines were fabricated in this way and used to immobilise polymer nanoparticles in 46 nm wide lines. Alternatively, the patterned monolayer may be used as a resist for wet etching of the metal substrate. Exquisite control of feature size may be affected in the range 46–126 nm, for single exposures, simply by varying the exposure time. For orthogonal exposures, structures as small as 35 nm (λ/7) could be formed in regular, square arrays with very low defect densities.

Acknowledgements

GT, DGL and GJL thank EPSRC (grants EP/D064767/1 and GR/C523857/1) for financial support. OEZ thanks the Libyan Government for a Research Scholarship. GPL and SRJB thank the National Science Foundation (grant 0515684) and the Office of Naval Research (grant N00014-10-1-0907) for financial support.

References

1 J. Sagiv, *J. Am. Chem. Soc.*, 1980, **102**, 92–98.
2 L. Netzer and J. Sagiv, *J. Am. Chem. Soc.*, 1983, **105**, 674–676.
3 R. G. Nuzzo and D. L. Allara, *J. Am. Chem. Soc.*, 1983, **105**, 4481–4483.
4 R. G. Nuzzo, F. A. Fusco and D. L. Allara, *J. Am. Chem. Soc.*, 1987, **109**, 2358–2368.
5 C. D. Bain, E. B. Troughton, Y.-T. Tao, J. Evall, G. M. Whitesides and R. G. Nuzzo, *J. Am. Chem. Soc.*, 1989, **111**, 321–335.
6 J. C. Love, L. A. Estroff, J. K. Kriebel, R. G. Nuzzo and G. M. Whitesides, *Chem. Rev.*, 2005, **105**, 1103–1170.
7 J. G. van Alsten, *Langmuir*, 1999, **15**, 7605.
8 W. Gao, L. Dickinson, C. Grozinger, F. G. Morin and L. Reven, *Langmuir*, 1996, **12**, 6429.
9 C. Viornery, Y. Chevolot, D. Leonar, B. Aronsson, P. Pechy, H. J. Mathieu, P. Descouts and M. Graetzel, *Langmuir*, 2002, **18**, 2582.
10 S. Tosatti, R. Michel, M. Textor and N. D. Spencer, *Langmuir*, 2002, **18**, 3537–3548.
11 R. A. Neves, M. E. Salmon, P. E. Russell and E. B. Troughton, *Langmuir*, 2000, **16**, 2409.
12 R. A. Neves, E. B. Troughton and P. E. Russell, *Nanotechnology*, 2001, **12**, 285.
13 X. Wang, M. Fujimaki and K. Awazu, *Opt. Express*, 2005, **13**, 1486.
14 J. E. G. J. Wijnhoven and W. L. Vos, *Science*, 1998, **281**, 802.
15 A. M. Adawi, A. R. A. Chalcraft, D. M. Whittaker and D. G. Lidzey, *Opt. Express*, 2007, **15**, 14299.
16 B. Li, X. Cai and Y. Zhang, *Appl. Phys. Lett.*, 2006, **89**, 031103.
17 B. O'Regan and M. Gratzel, *Nature*, 1991, **353**, 737–740.
18 A. Fujishima and K. Honda, *Nature*, 1975, **238**, 37–38.
19 S. A. Shevlin and S. M. Woodley, *J. Phys. Chem. C*, 2010, **114**, 17333–17343.
20 Y. Wang, D. Zhao, H. Ji, G. Liu, C. Chen, W. Ma, H. Zhu and J. Zhao, *J. Phys. Chem. C*, 2010, **114**, 17728–17733.
21 H. Haick and Y. Paz, *J. Phys. Chem. B*, 2001, **105**, 3045–3054.
22 H. Haick and Y. Paz, *Chem. Phys. Chem.*, 2003, **4**, 617–620.
23 R. Wang, K. Hashimoto, A. Fujishima, M. Chikuni, E. Kojima, A. Kitamura, M. Shimohigoshi and T. Watanabe, *Nature*, 1997, **388**, 431–432.
24 S.-Y. Ryu, D. S. Kim, J.-D. Jeon and S.-Y. Kwak, *J. Phys. Chem. C*, 2010, **114**, 17440–17445.
25 L. B. Goetting, T. Deng and G. M. Whitesides, *Langmuir*, 1999, **15**, 1182–1191.
26 N. Gadegaard, X. Chen, F. J. M. Rutten and M. R. Alexander, *Langmuir*, 2008, **24**, 2057–2063.
27 S. Sun and G. J. Leggett, *Nano Lett.*, 2007, **7**, 3753–3758.
28 P. Vettiger, M. Despont, U. Drechsler, U. Durig, W. Haberle, M. I. Lutwyche, H. Rothuizen, R. Stuts, R. Widmer and G. K. Binnig, *IBM J. Res. Dev.*, 2000, **44**, 323–340.
29 K. Salaita, Y. Wang, J. Fragala, R. A. Vega, C. Liu and C. A. Mirkin, *Angew. Chem., Int. Ed.*, 2006, **45**, 7220–7223.
30 E. u. Haq, Z. Liu, Y. Zhang, S. A. A. Ahmad, L.-S. Wong, S. P. Armes, J. K. Hobbs, G. J. Leggett, J. Micklefield, C. J. Roberts and J. M. R. Weaver, *Nano Lett.*, 2010, **10**, 4375–4380.
31 S. R. J. Brueck, *Proc. IEEE*, 2005, **93**, 1704–1721.
32 C. Lu and R. H. Lipson, *Laser Photonics Rev.*, 2009, 1–13.
33 S. Friebel, J. Aizenberg, S. Abad and P. Wiltzius, *Appl. Phys. Lett.*, 2000, **77**, 2406–2408.
34 T. Geldhauser, P. Leiderer, J. Boneberg, S. Walheim and T. Schimmel, *Langmuir*, 2008, **24**, 13155–13160.
35 C. Schuh, S. Santer, O. Prucker and J. Ruhe, *Adv. Mater.*, 2009, **21**, 4706–4710.
36 A. Turchanin, M. Schnietz, M. El-Desawy, H. H. Solak, C. David and A. Golzhauser, *Small*, 2007, **3**, 2114–2119.
37 N. Blondiaux, S. Zurcher, M. Liley and N. D. Spencer, *Langmuir*, 2007, **23**, 3489–3494.
38 G. Tizazu, A. Adawi, G. J. Leggett and D. G. Lidzey, *Langmuir*, 2009, **25**, 10746–10753.
39 R. Overney and E. Meyer, *MRS Bull.*, 1993, 26–34.
40 R. W. Carpick and M. Salmeron, *Chem. Rev.*, 1997, **97**, 1163–1194.

41 E. Gnecco, R. Bennewitz, T. Gyalog and E. Meyer, *J. Phys.: Condens. Matter*, 2001, **13**, R619.
42 G. J. Leggett, N. J. Brewer and K. C. Chong, *Phys. Chem. Chem. Phys.*, 2005, **7**, 1107–1120.
43 L. Novotny and B. Hecht, *Nanophotonics*, Cambridge University Press, Cambridge, UK, 2005.
44 M. A. Sillanpaa and P. J. Hakonen, *Physica E*, 2002, **14**, 41–47.
45 C. J. Boxley, H. S. White, C. E. Gardner and J. V. Macpherson, *J. Phys. Chem. B*, 2003, **107**, 9677–9680.
46 J. N. Anker, W. P. Hall, O. Lyandres, N. C. Shah, J. Zhao and R. P. Van Duyne, *Nat. Mater.*, 2008, **7**, 442–453.

